

Antibacterial Mesoporous Silica Granules Containing a Stable N-Halamine Moiety

Yuqing Shi, Haidong Xu, Yijing He, Xuan Tang, Hongru Tian, and Jie Liang*

Cite This: *ACS Omega* 2023, 8, 21410–21417

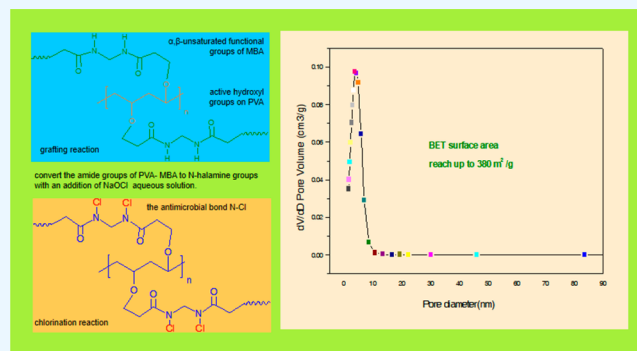
Read Online

ACCESS |

Metrics & More

Article Recommendations

ABSTRACT: High-efficacy and regenerable antimicrobial silica granules were prepared via oxa-Michael addition between poly(vinyl alcohol) (PVA) and methylene-bis-acrylamide (MBA) under the catalysis of sodium carbonate in an aqueous solution. Diluted water glass was added, and the solution pH was adjusted to about 7 to precipitate PVA-MBA modified mesoporous silica (PVA-MBA@SiO₂) granules. N-Halamine-grafted silica (PVA-MBA-Cl@SiO₂) granules were achieved by adding diluted sodium hypochlorite solution. It was found that a BET surface area of about 380 m² g⁻¹ for PVA-MBA@SiO₂ granules and a Cl⁺% of about 3.80% for PVA-MBA-Cl@SiO₂ granules could be achieved under optimized preparation conditions. Antimicrobial tests showed that the as-prepared antimicrobial silica granules were capable of about a 6-log inactivation of *Staphylococcus aureus* and *Escherichia coli* O157:H7 within 10 min of contact. Furthermore, the as-prepared antimicrobial silica granules can be recycled many times due to the excellent regenerability of their N-halamine functional groups and can be saved for a long time. With the above-mentioned advantages, the granules have potential applications in water disinfection.



1. INTRODUCTION

The outbreak of the coronavirus disease (COVID-19) pandemic has raised global public health awareness, which has caused more than 400 million confirmed cases and 6 million deaths worldwide. It is still increasing, causing immeasurable pain and economic losses.^{1,2} Microbial contamination and infection caused by pathogens are becoming more and more serious. Disinfection and sterilization are commonly used to prevent microbial proliferation and pathogen transmission. At present, the lack of clean drinking water has become a serious challenge for many countries in the world.³ In the field of water purification, microbial contamination remains one of the most serious problems.^{4,5} Commonly used water disinfection methods in the past few decades include free halogens, ozone, chloramine, and ultraviolet light.^{6,7} However, these disinfection methods have some disadvantages. Free chlorine, ozone, and chloramine are strong oxidants, which may react with organic impurities in water to form undesirable byproducts during disinfection of drinking water.^{8,9} Ultraviolet light does not have long-lasting sterilization ability and may lead to secondary microbial contamination of disinfected water.¹⁰

Over the past few decades, more and more researchers in related fields have paid attention to N-halamine antimicrobial materials since they have very strong antimicrobial activities, wide antibacterial spectra, and renewability of N-halamine

antibacterial functional groups.^{11–13} Dr. Worley's group prepared porous cross-linked N-halamine antibacterial beads for drinking water disinfection.^{14,15} Due to the high number of N-halamine moieties, these antimicrobial resins have strong antibacterial efficacies. Commercially speaking, these resins have the potential to become sterilizing filter materials in water purifiers. Nevertheless, these antimicrobial resins come with several shortcomings, such as high production costs and large amounts of waste organic solvents produced in the production process. Our research group made an improvement a few years ago by eliminating the use of organic solvents in the synthesis of a N-halamine antimicrobial polymeric resin.¹⁶ Although the synthesized resin has strong antibacterial effects, the stability of its N-halamine functional group still has room for improvement. Therefore, we need to further develop some environmentally friendly methods to prepare some powerful water-insoluble N-halamine materials with a stable and high content of oxidative halogen for water disinfection.

Received: June 29, 2022

Accepted: November 18, 2022

Published: June 5, 2023



Mesoporous silica which has a large specific surface area with highly ordered pores and a narrow pore size distribution has been widely used in the fields of separation, catalysis, drug delivery, and nanosensors, etc.^{17–20} Due to its large surface area, porous structure, very good thermal stability, and hydrophilicity, silica has the potential to be prepared as a water treatment and antimicrobial material. There have been some reports about N-halamine-modified mesoporous silica antimicrobial materials.^{21,22} The obtained mesoporous silica containing N-halamine moieties has good antibacterial activities. However, their preparation methods are complicated and need to be carried out in an organic solvent, resulting in relatively expensive production costs and waste organic solvents, which is disadvantageous for large-scale production and commercial applications. In this paper, we developed a facile, low-cost, green process for the preparation of antibacterial mesoporous silica granules containing a stable noncyclic N-halamine moiety (PVA-MBA-Cl@SiO₂ granules). The preparation process for PVA-MBA-Cl@SiO₂ granules is shown in Figure 1. Cheap and commercially available

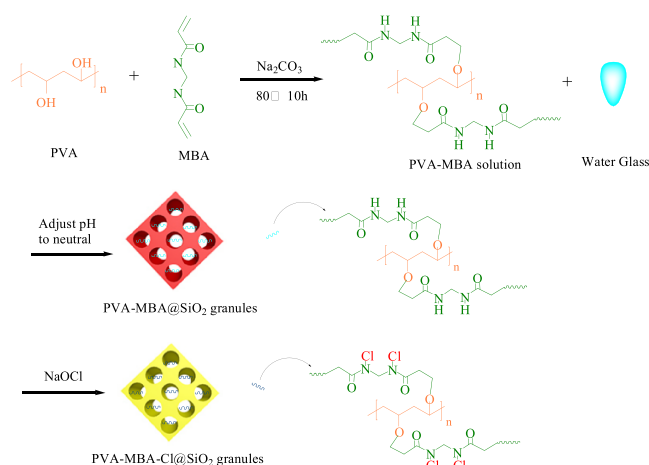


Figure 1. Preparation process for PVA-MBA-Cl@SiO₂ granules.

poly(vinyl alcohol) (PVA), methylene-bis-acrylamide (MBA), water glass, and sodium hypochlorite solution were used as raw materials. PVA and MBA reacted to form a polymer containing both hydroxy and amide groups (PVA-MBA) via the oxo-Michael addition between the active hydroxyl groups on PVA and α,β -unsaturated functional groups of MBA under the catalysis of sodium carbonate in an aqueous solution. The diluted water glass was added into the above PVA-MBA aqueous solution, and then the solution pH was adjusted to precipitate PVA-MBA modified mesoporous silica (PVA-MBA@SiO₂) granules. After simple chlorination in NaOCl solution, PVA-MBA-Cl@SiO₂ granules were formed via converting the amide groups in PVA-MBA@SiO₂ granules into N-halamine ones. With a large specific surface area, a high oxidative chlorine content, and stable N-halamine antibacterial groups, the obtained PVA-MBA-Cl@SiO₂ granules exhibit very good antibacterial efficacies and will have potential applications in water disinfection.

2. EXPERIMENTAL SECTION

2.1. Materials. Methylene-bis-acrylamide (MBA) and poly(vinyl alcohol) (PVA)1799 were bought from Macleans Shanghai Reagent Co., Ltd. Sulfuric acid, hydrochloric acid,

sodium carbonate, potassium iodide, and 7.5% NaOCl solution were purchased from Sinopharm Chemical Reagent Co., Ltd. Water glass (Na₂O₃·3SiO₂) 34 wt % was purchased from Shandong Yousuo Chemical Co., Ltd. *Staphylococcus aureus* (*S. aureus*) ATCC 25922 and *Escherichia coli* (*E. coli*) O157:H7 ATCC 941 were provided by Shanghai Institute of Materia Medica, Chinese Academy of Sciences.

2.2. Characterization. A JEOL 2100 transmission electron microscope was used to obtain transmission electron microscope (TEM) images. A PerkinElmer PHI 5000 ESCA system was used to obtain X-ray photoelectron spectroscopy (XPS) spectra. X-ray diffraction (XRD) spectra were gained by using Dmax-2000 X-ray diffraction. Fourier-transform infrared spectroscopy (FT-IR) spectra were obtained by a Thermo Scientific NicoletN10 infrared spectrometer. A Nova 4000e Surface Area and Pore Size Analyzer was adopted to acquire Brunauer–Emmett–Teller (BET) data.

2.3. Preparation of PVA-MBA@SiO₂ Granules. 0.30 g of Na₂CO₃, 0.30 g of PVA, and 0.30 g of MBA were added to 50 mL of deionized water, and reacted at 80 °C for 10 h. After cooling to about 30 °C, 3.80 g of water glass was diluted with 10 mL of deionized water and added to the above PVA-MBA reaction solution. The PVA-MBA@SiO₂ granules were obtained by adjusting the pH with 4 mol L⁻¹ hydrochloric acid to about 6.7, and the entire acid addition rate was fast to prevent the solution from gelling. The obtained crude PVA-MBA@SiO₂ granules were thoroughly rinsed with deionized water 3 times and then dried under a vacuum at 100 °C for 6 h.

2.4. Chlorination and Titration Analysis. PVA-MBA@SiO₂ granules (1.00 g) were added to 50 mL of deionized water, and then 5.0 mL of 7.5% NaOCl dilute solution was added dropwise under stirring with a pH adjustment to about 7.5 by using 0.50 mol L⁻¹ H₂SO₄. After the reaction mixture was stirred for 2 h under room temperature, PVA-MBA-Cl@SiO₂ granules were filtrated out and rinsed repeatedly with deionized water to remove residual hypochlorite ions and then dried under a vacuum at 50 °C for 2 h. The oxidative chlorine content (Cl⁺%) of PVA-MBA-Cl@SiO₂ granules could be measured by an iodometric method.^{23,24} The specific steps are as follows. A certain amount of PVA-MBA-Cl@SiO₂ granules were ground into a fine powder and accurately weighed. The weighed powders were transferred into an Erlenmeyer flask containing 50 mL of deionized water, and then 0.20 g of KI and 1.0 mL of 0.50 mol L⁻¹ H₂SO₄ were added. Finally, the solution was titrated with a 0.0100 mol L⁻¹ Na₂S₂O₃, and the end point of the titration was judged by a starch indicator. The Cl⁺% can be calculated as follows:

$$\text{Cl}^+(\%) = \frac{N \times V \times 35.45}{W \times 2} \times 100\%$$

where *N* is the molar concentration of Na₂S₂O₃ consumed (mol L⁻¹), *V* is the volume of Na₂S₂O₃ consumed (L), and *W* is the mass (g) of PVA-MBA-Cl@SiO₂ granules.

2.5. Storage Stability and Renewability Tests in PVA-MBA-Cl@SiO₂ Granules. The storage stability of N-halamine functional groups in PVA-MBA-Cl@SiO₂ granules can be evaluated by measuring the change in the Cl⁺% of PVA-MBA-Cl@SiO₂ granules during the storage period.²⁵ The specific procedure is as follows: The Cl⁺% of the obtained PVA-MBA-Cl@SiO₂ granules was measured and stored in a dark environment at room temperature, and one portion was taken every 7 days for measurement of Cl⁺%. The N-halamine

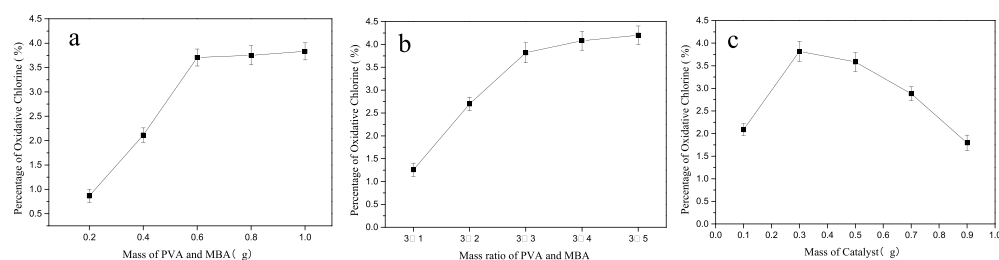


Figure 2. Influences of (a) the mass of PVA and MBA (the mass ratio of PVA and MBA: 1:1; the mass of catalyst: 0.30 g), (b) the mass ratio of PVA and MBA (the mass of PVA: 0.30 g; the mass of catalyst: 0.30 g), and (c) the mass of catalyst (the mass of PVA and MBA: 0.60 g; the mass ratio of PVA and MBA: 1:1) on the Cl^+ % of the as-prepared PVA-MBA-Cl@SiO₂ granules (the reaction temperature of PVA and MBA: 80 °C; the reaction time of PVA and MBA: 10 h; the mass of the water glass: 3.80 g; solvent: 50 mL of water).

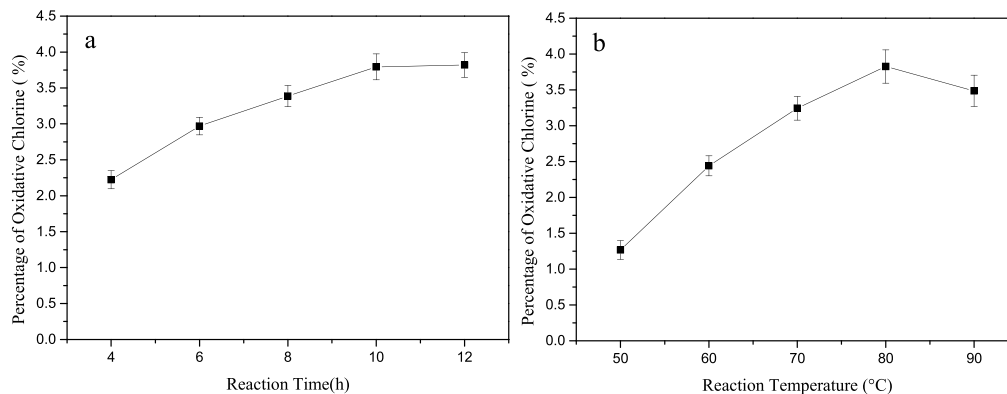


Figure 3. Influences of (a) reaction time (reaction temperature: 80 °C) and (b) reaction temperature (reaction time: 10 h) on the Cl^+ % of the as-prepared PVA-MBA-Cl@SiO₂ granules (catalyst amount: 0.30 g; the mass of the water glass: 3.80 g; the mass ratio of PVA and MBA: 1:1; mass of PVA and MBA: 0.60 g; solvent: 50 mL of water).

functional group in the PVA-MBA-Cl@SiO₂ granules was reduced with a reducing agent and then regenerated, and the Cl^+ on the regenerated PVA-MBA-Cl@SiO₂ granules was measured. This procedure was repeated several times, and the renewability of the antibacterial functional group in the PVA-MBA-Cl@SiO₂ granules was judged according to the change of Cl^+ %.²⁶ A Na₂S₂O₃ aqueous solution (0.03 mol L⁻¹) was prepared, and then 3.00 g of the as-prepared PVA-MBA-Cl@SiO₂ granules was transferred to 100 mL of a 0.03 mol L⁻¹ aqueous Na₂S₂O₃ solution, and stirred at room temperature for 1 h to fully annihilate oxidized chlorine of PVA-MBA-Cl@SiO₂ granules. The reduced granules were filtered out and washed thoroughly to remove residual sodium thiosulfate and then rechlorinated with the addition of NaOCl solution. The Cl^+ % of PVA-MBA-Cl@SiO₂ after rechlorination was tested. This procedure was repeated 10 times, and the renewability of the N-halamine group in PVA-MBA-Cl@SiO₂ granules was determined by the change in Cl^+ %.

2.6. Antibacterial Performance Test^{27,28} of PVA-MBA-Cl@SiO₂ Granules. *E. coli* and *S. aureus* were adopted to investigate the bactericidal properties of PVA-MBA-Cl@SiO₂ granules in water. The specific procedure is as follows. The weighed sample (0.50 g) was ultrasonically dispersed in 50 mL of sterile phosphate buffer saline (PBS) solution, and then the bacterial solution was added to the above mixture. After oscillation at 37 °C for a certain amount of time to allow the sample to fully contact the bacterial solution, 0.50 mL of the upper bacterial suspension was taken out and added to a test tube containing 4.0 mL of PBS and 0.5 mL of 0.1 mol L⁻¹ sodium thiosulfate. The resulting mixture was serially diluted with PBS, and 100 μL of each dilution was distributed onto the

agar plate medium. After incubation at 37 °C for 24 h, the colonies on the agar plate were counted.

3. RESULTS AND DISCUSSION

3.1. Preparation of the PVA-MBA-Cl@SiO₂ Granules.

With poly(vinyl alcohol) (PVA) and methylene-bis-acrylamide (MBA) as raw materials, a polymer containing N-halamine precursor functional groups (PVA-MBA) can be obtained via the oxa-Michael addition between the active hydroxyl groups on PVA and the α,β -unsaturated functional groups of MBA under the catalysis of sodium carbonate in an aqueous solution.²⁹ In this study, we tried to develop antibacterial mesoporous silica granules containing stable N-halamine moieties, which can be used as a disinfectant in water. For this purpose, we chose water glass as the silicon source to prepare antibacterial mesoporous silica granules. After the diluted water glass was added to the PVA-MBA aqueous solution, PVA-MBA modified mesoporous silica (PVA-MBA@SiO₂) precipitation could be obtained via adjusting pH of the solution to about 6–7. The precipitate was washed and dried to obtain PVA-MBA@SiO₂ granules. It is well-known that the isoelectric point (pI) of orthosilicic acid is about 2, so under neutral conditions, the silicates are negatively charged. According to the cooperative formation mechanism proposed by Stucky et al.,^{30,31} the formation process of PVA-MBA@SiO₂ is a S⁰X-mechanism, and negatively charged silicates (X⁻) and electrical neutral PVA-MBA molecules (S⁰) are combined by electrostatic force and hydrogen bonding. The antibacterial mesoporous silica (PVA-MBA-Cl@SiO₂) granules could be formed via chlorinating the amide group of PVA-MBA@SiO₂ in NaOCl solution. In order to obtain a higher oxidative

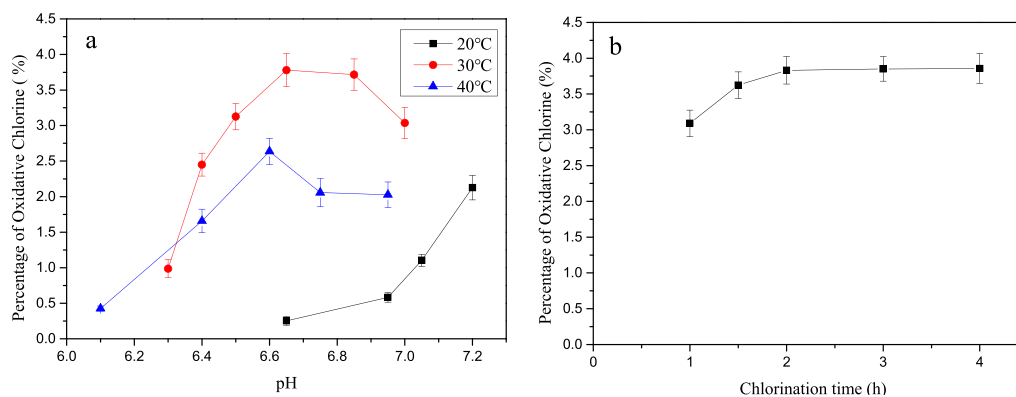


Figure 4. Effects of (a) precipitating pH under different temperatures and (b) chlorination time on Cl⁺% of the obtained PVA-MBA-Cl@SiO₂ granules.

chlorine content (Cl⁺%) in the as-prepared PVA-MBA-Cl@SiO₂ granules, we investigated the effects of the mass of PVA and MBA, the mass ratio of PVA and MBA, the mass of catalyst, the reaction temperature of PVA and MBA, the reaction time of PVA and MBA, the temperature and pH of the solution during precipitation, and the chlorination time on the Cl⁺% of the as-prepared PVA-MBA-Cl@SiO₂ granules.

The influences of the mass of PVA and MBA, the mass ratio of PVA and MBA, and the mass of catalyst on the Cl⁺% of the

surface of SiO₂ precipitate. Therefore, more added PVA and MBA cannot further increase the Cl⁺%. As shown in Figure 2b, the Cl⁺% increased from 1.25% to 3.80% with the mass ratio of MBA/PVA increased from 1:3 to 1:1. Further increasing the mass ratio of MBA/PVA only caused a small increase in Cl⁺%. Figure 2c shows the effect of the mass of catalyst on Cl⁺% of the as-prepared PVA-MBA-Cl@SiO₂ granules. Na₂CO₃ is a suitable catalyst for pxa-Michael addition.³² In this study, we adopted Na₂CO₃ as the catalyst for the oxa-Michael addition between PVA and MBA. As shown in Figure 2c, the Cl⁺% of the as-prepared PVA-MBA-Cl@SiO₂ granules increased from 2.08% to 3.82% with the mass of catalyst increasing from 0.10 to 0.30 g. However, when the mass of catalyst was further increased from 0.30 to 0.90 g, the Cl⁺% substantially decreased from 3.82% to 1.79%. A possible reason for this decrease is that too much added Na₂CO₃ causes an increase of the solution pH to a certain level, which is not conducive to the reaction between PVA and MBA.³³ Therefore, the optimal added mass of PVA and MBA, mass ratio of PVA and MBA, and mass of catalyst were 0.60 g, 1:1, and 0.30 g with an addition of 3.80 g of water glass, respectively.

Figure 3 displays the influences of reaction temperature and time of PVA and MBA on Cl⁺% of the as-prepared PVA-MBA-Cl@SiO₂ granules. As seen in Figure 3a, the Cl⁺% of the obtained PVA-MBA-Cl@SiO₂ granules increased from 2.22% to 3.79% with a prolonged reaction time of PVA and MBA from 4 to 10 h, and further prolonging the reaction time from 10 to 12 h did not make the Cl⁺% increase a lot. As seen in Figure 3b, the Cl⁺% increased from 1.27% to 3.83% with the reaction temperature rise from 50 to 80 °C. However, further increasing the reaction temperature from 80 to 90 °C resulted in a decline of Cl⁺% from 3.83% to 3.49%, indicating that too high a temperature is not favorable for the formation of PVA-MBA molecules. Therefore, 10 h and 80 °C were chosen as the optimized reaction time and temperature of PVA and MBA.

During our study, we found that the solution pH is very sensitive to the precipitation of PVA-MBA@SiO₂ granules. The effects of the precipitation pH under three different temperatures and chlorination time on the Cl⁺% of the as-prepared PVA-MBA-Cl@SiO₂ granules are displayed in Figure 4. Since the water glass is strongly alkaline and the pH of the mixed solution of glass water and PVA-MBA is above 11, 4 mol L⁻¹ HCl was used to decrease the pH for the precipitation of PVA-MBA@SiO₂ granules. As displayed in Figure 4a, under 20 °C, PVA-MBA@SiO₂ granules began to precipitate out at pH 7.20. The Cl⁺% of the obtained PVA-MBA-Cl@SiO₂ granules

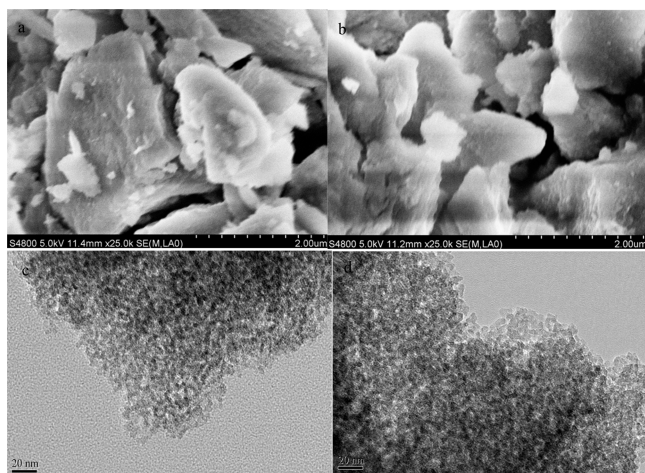


Figure 5. SEM images of (a) PVA-MBA@SiO₂ and (b) PVA-MBA-Cl@SiO₂ granules, TEM images of (c) PVA-MBA@SiO₂ and (d) PVA-MBA-Cl@SiO₂ granules.

obtained PVA-MBA-Cl@SiO₂ granules are demonstrated in Figure 2. As shown in Figure 2a, we kept the mass of the water glass (3.80 g) and the mass ratio of PVA and MBA (1:1) constant and gradually changed the mass of PVA and MBA. It was found that the Cl⁺% of the as-prepared PVA-MBA-Cl@SiO₂ granules was raised substantially from 0.83% to 3.71% with the increase of the mass of PVA and MBA from 0.20 to 0.60 g. When the mass of PVA and MBA continued to increase from 0.60 to 1.00 g, the Cl⁺% only changed a little. It is reasonable that more PVA and MBA molecules can lead to more amide functional groups fixed on the surface of SiO₂ precipitate via a S⁰X-mechanism, resulting in higher Cl⁺% after chlorination of amide groups. However, as the number of PVA-MBA molecules exceeds that of the negatively charged silicates (X⁻), the extra PVA-MBA molecules cannot be fixed on the

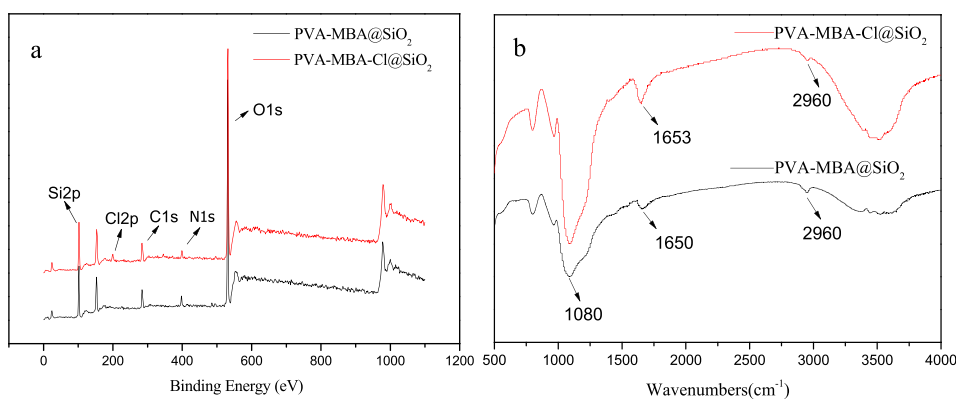


Figure 6. XPS spectra (a) and FT-IR (b) of PVA-MBA@SiO₂ and PVA-MBA-Cl@SiO₂ granules.

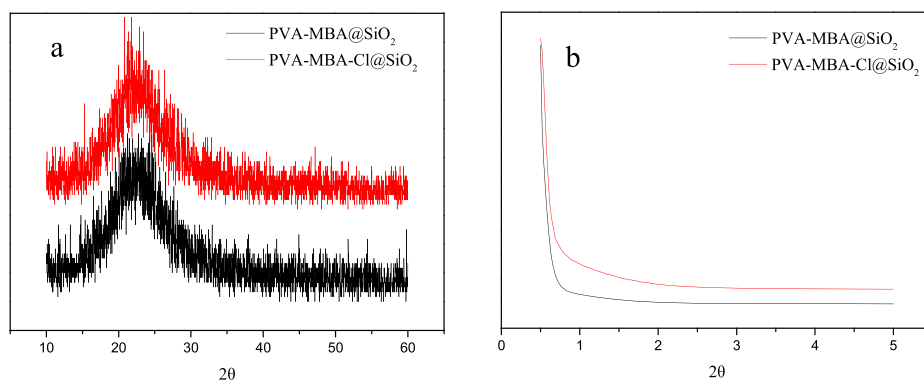


Figure 7. XRD (a) and SXRD (b) diffraction patterns of PVA-MBA@SiO₂ and PVA-MBA-Cl@SiO₂ granules.

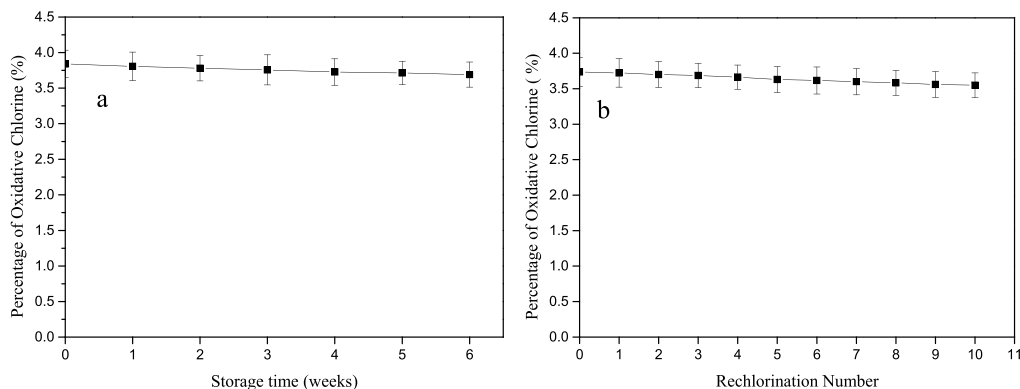


Figure 8. (a) N₂ adsorption–desorption isotherm and (b) pore size distribution curve of PVA-MBA@SiO₂ granules.

substantially decreased from 2.12% to 0.25% with the precipitation pH decreasing from 7.20 to 6.65. Under 30 °C, PVA-MBA@SiO₂ granules began to precipitate out at pH 7.00. The Cl⁺% of the obtained PVA-MBA-Cl@SiO₂ granules gradually increased from 3.04% to 3.78% with the precipitation pH decreased from 7.00 to 6.65 and then substantially decreased from 3.78% to 0.99% with the precipitation pH decreased from 6.65 to 6.30. Under 40 °C, PVA-MBA@SiO₂ granules began to precipitate out at pH 6.95. The Cl⁺% of the obtained PVA-MBA-Cl@SiO₂ particles gradually increased from 2.03% to 2.64% with the precipitation pH decreased from 6.95 to 6.55 and then substantially decreased from 2.64% to 0.43% with the precipitation pH decreased from 6.55 to 6.10. It is very clear that the optimal precipitation pH and temperature are 6.65–6.85 and 30 °C. As seen in Figure 4b, the Cl⁺% of PVA-MBA-Cl@SiO₂ increased with prolonging

the chlorination time and was 3.84% at 2 h. After 2 h, further prolonging the time did not change the Cl⁺%. It is very clear that 2 h is the optimized chlorination time.

3.2. Characterization of PVA-MBA-Cl@SiO₂ Granules.

3.2.1. SEM and TEM. The SEM and TEM of PVA-MBA@SiO₂ and PVA-MBA-Cl@SiO₂ granules are shown in Figure 5. The as-prepared PVA-MBA@SiO₂ and PVA-MBA-Cl@SiO₂ granules were microstructures of particle packing, and chlorination had no significant effect on the material structure in Figure 5a,b. The as-prepared PVA-MBA@SiO₂ and PVA-MBA-Cl@SiO₂ granules did not show a common ordered pore structure in Figure 5c,d. The TEM image was very similar to the typical disordered mesoporous silica.³⁴ After chlorination, there was no significant change in the pore structure.

3.2.2. XPS and FT-IR Spectra. XPS and FT-IR spectra of PVA-MBA@SiO₂ and PVA-MBA-Cl@SiO₂ granules are shown

in Figure 6. Both PVA-MBA@SiO₂ and PVA-MBA-Cl@SiO₂ granules in Figure 6a show signals of nitrogen (N 1s: 399.97 eV) and carbon (C 1s: 284.57 eV), indicating the existence of carbon and nitrogen atoms in the prepared silica materials, which proved the successful combination of PVA-MBA and silica. Compared with PVA-MBA@SiO₂ granules, PVA-MBA-Cl@SiO₂ granules had a new peak of chlorine (Cl 2p: 200.3 eV), which was ascribed to the existence of N–Cl bonds in PVA-MBA-Cl@SiO₂ granules.³⁵ As shown in Figure 6b, the peak at 2960 cm⁻¹ is caused by a stretching vibration of the C–H group,³⁶ indicating that PVA-MBA is bound to silica. After chlorination, the peak of amide C=O stretching vibration shifts from 1650 to 1653 cm⁻¹ due to the electron-withdrawing effect of the adjacent oxidative chlorine.³⁷

3.2.3. XRD and SXRD Spectra. X-ray diffraction (XRD) and small angle XRD (SXRD) can be adopted to determine the crystal structure and pore structure of porous materials. As shown in Figure 7a, the large angle XRD diffraction pattern ($2\theta = 10\text{--}60^\circ$) indicates that both PVA-MBA@SiO₂ and PVA-MBA-Cl@SiO₂ granules are typical amorphous phase structures. As shown in Figure 7b, both PVA-MBA@SiO₂ and PVA-MBA-Cl@SiO₂ particles have no obvious SXRD diffraction peaks, indicating that they may have disordered pore structures.³⁸ This result corresponds to the result of TEM.

3.2.4. BET Surface Area. The nitrogen adsorption/desorption isotherm and pore size distribution curve of PVA-MBA@SiO₂ granules are presented in Figure 8, and the results of BET surface area, pore volume, and pore diameter of PVA-MBA@SiO₂ granules are summarized in Table 1. Figure 8a

Table 1. Surface Area, Pore Volume, and Pore Diameter of PVA-MBA@SiO₂ Granules

sample	BET surface area (m ² g ⁻¹)	volume of pores (cm ³ g ⁻¹)	pore diameter (nm)
PVA-MBA@SiO ₂	380	0.44	4.1

shows a type IV isotherm with H₂ hysteresis loops in the relative pressure range of 0.4 to 0.8 according to the standard classification of isotherms. Type IV adsorption isotherms were considered to be typical adsorption isotherms for mesoporous materials.³⁹ From Figure 8b, we could also see that PVA-MBA@SiO₂ particles had a uniform distribution of pore size. The BET surface area of PVA-MBA@SiO₂ granules could

reach up to 380 m² g⁻¹, which is good for its application in disinfection of water.

3.3. Performance Evaluation of PVA-MBA-Cl@SiO₂ Granules. **3.3.1. Storage Stability and Renewability in PVA-MBA-Cl@SiO₂ Granules.** The storage stability and renewability of N-halamine groups in PVA-MBA-Cl@SiO₂ granules are shown in Figure 9. As seen in Figure 9a, the Cl⁺% of the obtained PVA-MBA-Cl@SiO₂ granules decreased slightly from 3.84% to 3.69% after storage under room temperature for 6 weeks, demonstrating that the antibacterial N-halamine groups in PVA-MBA-Cl@SiO₂ granules are very stable. From Figure 9b, it could be found that after 10 times of rechlorination, the Cl⁺% of the obtained PVA-MBA-Cl@SiO₂ granules only decreased from initial 3.74% to 3.55%, which means very good renewability of N-halamine groups in PVA-MBA-Cl@SiO₂ granules.

3.3.2. Antibacterial Performance of PVA-MBA-Cl@SiO₂ Granules. The antibacterial performance of PVA-MBA@SiO₂ and PVA-MBA-Cl@SiO₂ was tested with *S. aureus* and *E. coli*. The results are displayed in Table 2. For PVA-MBA@SiO₂

Table 2. Antibacterial Performance of PVA-MBA@SiO₂ and PVA-MBA-Cl@SiO₂ Granules against *E. coli* and *S. aureus*

sample	contact time (min)	<i>S. Aureus</i> ^a reduction (%)	<i>E. coli</i> ^b reduction (%)
PVA-MBA@SiO ₂	10	11.00	15.00
PVA-MBA-Cl@SiO ₂ (Cl ⁺ % = 3.81%)	1	98.16	98.59
	5	99.36	99.49
	10	100	100

^aInoculum was 2.07×10^6 colony forming units (CFU) per sample.

^bInoculum was 5.61×10^6 CFU per sample.

granules, only 11% and 15% of *S. aureus* and *E. coli* were inactivated within 10 min of contact. For PVA-MBA-Cl@SiO₂ granules, 98.16%, 99.36%, 100% and 98.59%, 99.49%, 100% of *S. aureus* and *E. coli*, respectively, were inactivated within 1, 5, 10 min of contact. Xu's group prepared antibacterial N-halamine decorated mesoporous silica nanoparticles which can inactivate 95% of *S. aureus* after 10 min of contact.⁴⁰ By comparison, it is clear that the as-prepared PVA-MBA-Cl@SiO₂ granules have strong antimicrobial efficacies.

4. CONCLUSIONS

In this research, a green and valuable two-step process was successfully developed for the preparation of antimicrobial

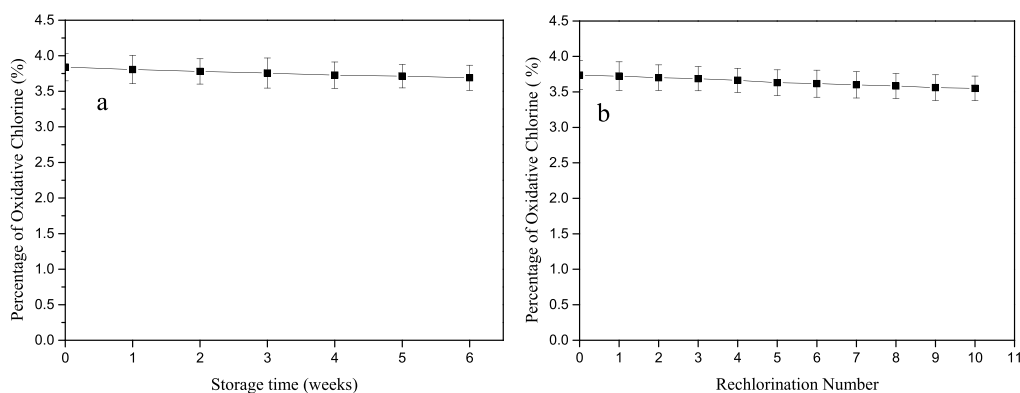


Figure 9. Storage stability (a) and renewability (b) of N-halamine groups in PVA-MBA-Cl@SiO₂ granules.

mesoporous silica granules modified with stable N-halamine moieties. In this preparation process, cheap and available water glass was chosen as an economical silica source for the preparation of mesoporous silica granules. Very interestingly, the existence of PVA-MBA molecules can lead to the rapid precipitation of mesoporous silica particles containing N-halamine precursor groups (amide groups) under a certain pH range. Compared to silica gels, the precipitated mesoporous silica (PVA-MBA@SiO₂) granules can be easily separated from the solution and dried due to less water content absorbed in these granules. Practically, in a large-scale production, after the filtration, the wet PVA-MBA@SiO₂ granules can be directly used for the chlorination of their amide groups to form antimicrobial mesoporous silica (PVA-MBA-Cl@SiO₂) granules without drying. The results showed that the obtained PVA-MBA-Cl@SiO₂ granules had uniform mesoporous channels and a large specific surface area. Furthermore, the obtained PVA-MBA-Cl@SiO₂ granules had strong antibacterial effects, good storage stability, and renewability of the N-halamine moiety. Therefore, the as-prepared antibacterial mesoporous silica granules will have a good application prospects in the field of water disinfection.

AUTHOR INFORMATION

Corresponding Author

Jie Liang – The Education Ministry Key Lab of Resource Chemistry and Shanghai Key Laboratory of Rare Earth Functional Materials, Shanghai Normal University, Shanghai 200234, P. R. China; orcid.org/0000-0002-3870-4199; Email: liangjie@shnu.edu.cn

Authors

Yuqing Shi – The Education Ministry Key Lab of Resource Chemistry and Shanghai Key Laboratory of Rare Earth Functional Materials, Shanghai Normal University, Shanghai 200234, P. R. China; orcid.org/0000-0002-8600-9123

Haidong Xu – The Education Ministry Key Lab of Resource Chemistry and Shanghai Key Laboratory of Rare Earth Functional Materials, Shanghai Normal University, Shanghai 200234, P. R. China

Yijing He – The Education Ministry Key Lab of Resource Chemistry and Shanghai Key Laboratory of Rare Earth Functional Materials, Shanghai Normal University, Shanghai 200234, P. R. China

Xuan Tang – The Education Ministry Key Lab of Resource Chemistry and Shanghai Key Laboratory of Rare Earth Functional Materials, Shanghai Normal University, Shanghai 200234, P. R. China

Hongru Tian – The Education Ministry Key Lab of Resource Chemistry and Shanghai Key Laboratory of Rare Earth Functional Materials, Shanghai Normal University, Shanghai 200234, P. R. China

Complete contact information is available at:

<https://pubs.acs.org/10.1021/acsomega.2c04079>

Notes

The authors declare no competing financial interest.

ACKNOWLEDGMENTS

The authors would like to acknowledge the financial support from the Shanghai Pujiang Talent Project (11PJ1407600).

This work is supported by PCSIRT (RT1269) and the Program of Shanghai Normal University (DZL124).

REFERENCES

- (1) Nagpal, A. S.; Mukai, A.; Sharma, S. Demonstrating the vital role of psychiatry throughout the health care continuum: Lessons learned from the impacts of the COVID-19 pandemic on pain management care. *J. Pm & R.* **2021**, *13* (6), 579.
- (2) Habib, S.; Alsanea, M.; Aloraini, M.; Al-Rawashdeh, H. S.; Islam, M.; Khan, S. An Efficient and Effective Deep Learning-Based Model for Real-Time Face Mask Detection. *Sensors* **2022**, *22* (7), 2602.
- (3) Wen, X.; Chen, F.; Lin, Y.; Zhu, H.; Yuan, F.; Kuang, D.; Jia, Z.; Yuan, Z. Microbial Indicators and Their Use for Monitoring Drinking Water Quality—A Review. *Sustainability* **2020**, *12* (6), 2249.
- (4) Mpundu, P.; Mbewe, A. R.; Muma, J. B.; Zgambo, J.; Munyeme, M. Evaluation of Bacterial Contamination in Dressed Chickens in Lusaka Abattoirs. *Frontiers in Public Health* **2019**, *7*, 19.
- (5) Kroll, S.; Brandes, C.; Wehling, J.; Treccani, L.; Grathwohl, G.; Rezwani, K. Highly efficient enzyme-functionalized porous zirconia microtubes for bacteria filtration. *Environmental science & technology*. **2012**, *46* (16), 8739–8747.
- (6) Sivarajani, K.; Sivakumar, S.; Dharmaraja, J. Enhancement Photocatalytic Activity of Mn Doped Cds/Zno Nanocomposites for the Degradation of Methylene Blue Under Solar Light Irradiation. *Advances in Materials Science* **2022**, *22* (2), 28.
- (7) Gao, M. Development of Photocatalytic Functional Coatings via Magnetron Sputtering Deposition and Their Integration into a Laboratory-Scale Water Treatment Reactor; Manchester Metropolitan University, 2022.
- (8) Jaffari, Z. H.; Abuabdou, S. M.A.; Ng, D.-Q.; Bashir, M. J.K. Insight into two-dimensional MXenes for environmental applications: Recent Progress, Challenges, and Prospects. *FlatChem* **2021**, *28*, 100256.
- (9) Apollaro, C.; Fuoco, I.; Criscuoli, A.; Figoli, A. Inorganic Pollutants into Groundwater: From Geochemistry to Treatment. *Geofluids* **2022**, *2022*, 9846802.
- (10) Munnawar, I.; Iqbal, S. S.; Anwar, M. N.; Batool, M.; Tariq, S.; Faima, N.; Khan, A. L.; Khan, A. U.; Nazar, U.; Jamil, T.; Ahmad, N. M. Synergistic effect of Chitosan-Zinc Oxide Hybrid Nanoparticles on antibiofouling and water disinfection of mixed matrix polyethersulfone nanocomposite membranes. *Carbohydrate Polymers* **2017**, *175*, 661–670.
- (11) Li, Y.; Liu, X.; Tan, L.; Cui, Z.; Yang, X.; Yeung, K.W. K.; Pan, H.; Wu, S. Construction of N-halamine labeled silica/zinc oxide hybrid nanoparticles for enhancing antibacterial ability of Ti implants. *Materials Science & Engineering C* **2017**, *76*, 50–58.
- (12) Wen, J.; Khan, A. D.; Sartorelli, J. B.; Goodyear, N.; Sun, Y. Aqueous-based continuous antimicrobial finishing of polyester fabrics to achieve durable and rechargeable antibacterial, antifungal, and antiviral functions. *Journal of Industrial and Engineering Chemistry* **2022**, *107*, 249–258.
- (13) Lan, S.; Zhang, J.; Li, J.; Guo, Y.; Sheng, X.; Dong, A. An N-Halamine/Graphene Oxide-Functionalized Electrospun Polymer Membrane That Inactivates Bacteria on Contact and by Releasing Active Chlorine. *Polymers* **2021**, *13* (16), 2784.
- (14) Chen, Y.; Worley, S. D.; Kim, J.; Wei, C.-I.; Chen, T.-Y.; Suess, J.; Kawai, H.; Williams, J. F. Biocidal Polystyrenehydantoin Beads. 2. Control of Chlorine Loading. *Ind. Eng. Chem. Res.* **2003**, *42* (23), 5715–5720.
- (15) Chen, Y.; Worley, S. D.; Kim, J.; Wei, C.-I.; Chen, T.-Y.; Santiago, J. I.; Williams, J. F.; Sun, G. Biocidal Poly(styrenehydantoin) Beads for Disinfection of Water. *Industrial & Engineering Chemistry Research* **2003**, *42* (2), 280–284.
- (16) Jie, Z.; Yan, X.; Zhao, L.; Worley, S. D.; Liang, J. Eco-friendly synthesis of regenerable antimicrobial polymeric resin with N-halamine and quaternary ammonium salt groups. *RSC Advances* **2014**, *4*, 6048–6054.
- (17) Li, M.; Liu, C.; Qi, L.; Liu, H. Nitrogen-Doped Graphene Quantum Dots Anchored on Hollow Zeolitic Imidazolate Frame-

- work-8 Colloidosomes for Fluorescence Detection of Glucose. *ACS Applied Nano Materials* **2022**, *5* (4), 5425–5438.
- (18) Luo, T.; Hua, C.; Liu, F.; Sun, Q.; Yi, Y.; Pan, X. Effect of adding solid waste silica fume as a cement paste replacement on the properties of fresh and hardened concrete. *Case Studies in Construction Materials* **2022**, *16*, e01048.
- (19) Wacht, D.; David, M.; Hinkov, B.; Detz, H.; Schwaighofer, A.; Baumgartner, B.; Lendl, B. Mesoporous Zirconia Coating for Sensing Applications Using Attenuated Total Reflection Fourier Transform Infrared (ATR FT-IR) Spectroscopy. *Applied spectroscopy* **2022**, *76* (1), 141–149.
- (20) Kim, G. W.; Han, I.-S.; Ha, J. W. Mesoporous silica shell-coated single gold nanorods as multifunctional orientation probes in dynamic biological environments. *RSC advances* **2021**, *11* (61), 38632–38637.
- (21) Hao, Y.; Wang, H.; Liu, S.; Chai, D.; Gao, G.; Hao, X. Multi-sites N-halamine antibacterial agent loaded on mesoporous silica nanoparticles with pH stimulus response. *Colloid and Interface Science Communications* **2022**, *46*, 100586.
- (22) Liu, Y.; Dong, X.; Bao, K.; Deng, Z.; Hossen, M. A.; Dai, J.; Qin, W.; Lee, K. Effective removal of cationic dyes in water by polyacrylonitrile/silica aerogel/modified antibacterial starch particles/zinc oxide beaded fibers prepared by electrospinning. *Journal of Environmental Chemical Engineering* **2021**, *9* (6), 106801.
- (23) Staneva, D.; Said, A. I.; Vasileva-Tonkova, E.; Grabchev, I. Enhanced Photodynamic Efficacy Using 1,8-Naphthalimides: Potential Application in Antibacterial Photodynamic Therapy. *Molecules* **2022**, *27* (18), 5743.
- (24) Jayme, S. B.; Prado, F. M.; Massafra, M. P.; Ronsein, G. E.; Di Mascio, P. Characterization and Quantification of Tryptophan and Tyrosine-Derived Hydroperoxides. *Photochem. Photobiol.* **2022**, *98* (3), 678–686.
- (25) Huang, K.; Yang, X.; Ma, Y.; Sun, G.; Nitin, N. Incorporation of Antimicrobial Bio-Based Carriers onto Poly(vinyl alcohol-co-ethylene) Surface for Enhanced Antimicrobial Activity. *ACS applied materials & interfaces* **2021**, *13* (30), 36275–36285.
- (26) Aguilar Sánchez, A. *Nanopolysaccharide Coatings for Functional Surfaces in Water-Treatment Materials: from Mechanisms to Process Scalability*. Department of Materials and Environmental Chemistry (MMK), Stockholm University, 2022.
- (27) Ghosh, N.; Sen, S.; Biswas, G.; Singh, L. R.; Chakdar, D.; Haldar, P. K. A comparative study of CuO nanoparticle and CuO/PVA-PVP nanocomposite on the basis of dye removal performance and antibacterial activity in wastewater treatment. *International Journal of Environmental Analytical Chemistry* **2022**, 1–21.
- (28) Demir, B.; Cerkez, I.; Worley, S. D.; Broughton, R. M.; Huang, T.-S. N-Halamine-modified antimicrobial polypropylene nonwoven fabrics for use against airborne bacteria. *ACS applied materials & interfaces* **2015**, *7* (3), 1752–1757.
- (29) Chen, X.; Wang, J. Degradation performance and mechanism of penicillin G in aqueous solution by ionizing radiation. *Journal of Cleaner Production* **2021**, *328*, 129625.
- (30) Huo, Q.; Margolese, D. I.; Ciesla, U.; Feng, P.; Gier, T. E.; Sieger, P.; Leon, R.; Petroff, P. M.; Schuth, F.; Stucky, G. D. Generalized synthesis of periodic surfactant/inorganic composite materials. *Nature* **1994**, *368*, 317–321.
- (31) Huo, Q.; Margolese, D. I.; Ciesla, U.; Demuth, D. G.; Feng, P.; Gier, T. E.; Sieger, P.; Firouzi, A.; Chmelka, B. F. Organization of Organic Molecules with Inorganic Molecular Species into Nano-composite Biphase Arrays. *Chem. Mater.* **1994**, *6* (8), 1176–1191.
- (32) Tian, H.; Zhai, Y.; Xu, C.; Liang, J. Durable Antibacterial Cotton Fabrics Containing Stable Acyclic N-Halamine Groups. *Industrial & Engineering Chemistry Research* **2017**, *56* (28), 7902–7909.
- (33) Kisanga, P. B.; Ilankumaran, P.; Fetterly, B. M.; Verkade, J. G. P(RNCH₂CH₂)₃N: Efficient 1,4-Addition Catalysts. *J. Org. Chem.* **2002**, *67* (11), 3555–3560.
- (34) Pauly, T. R.; Pinnavaia, T. J. Pore Size Modification of Mesoporous HMS Molecular Sieve Silicas with Wormhole Framework Structures. *Chemistry of Materials* **2001**, *13* (3), 987–993.
- (35) Wu, L.; Xu, Y.; Cai, L.; Zang, X.; Li, Z. Synthesis of a novel multi N-halamines siloxane precursor and its antimicrobial activity on cotton. *Applied Surface Science* **2014**, *314*, 832–840.
- (36) Prado, A. G. S.; Airoidi, C. A toxicity decrease on soil microbiota by applying the pesticide picloram anchored onto silica gel. *Green Chemistry* **2002**, *4* (3), 288–291.
- (37) Liu, Y.; Ma, K.; Li, R.; Ren, X.; Huang, T. S. Antibacterial cotton treated with N-halamine and quaternary ammonium salt. *Cellulose* **2013**, *20*, 3123–3130.
- (38) Chen, S.-Y.; Cheng, S. Acid-Free Synthesis of Mesoporous Silica Using Triblock Copolymer as Template with the Aid of Salt and Alcohol. *Chem. Mater.* **2007**, *19* (12), 3041–3051.
- (39) Kruk, M.; Jaroniec, M. Gas Adsorption Characterization of Ordered Organic–Inorganic Nanocomposite Materials. *Chem. Mater.* **2001**, *13*, 3169–3183.
- (40) Xu, J.; Zhang, Y.; Zhao, Y.; Zou, X. Antibacterial activity of N-halamine decorated mesoporous silica nanoparticles. *Journal of Physics and Chemistry of Solids* **2017**, *108*, 21–24.